This is a peer-reviewed, accepted author manuscript of the following research article: Yap, J. K. Y., Pickard, B. S., Gan, S. Y., & Chan, E. W. L. (2021). Genes associated with amyloid-beta-induced inflammasome-mediated neuronal death identified using functional gene trap mutagenesis approach. *International Journal of Biochemistry and Cell Biology*, *136*, [106014]. https://doi.org/10.1016/j.biocel.2021.106014

Genes Associated with Amyloid-beta-induced Inflammasome-mediated Neuronal Death Identified Using Functional Gene Trap Mutagenesis Approach

Jeremy Kean Yi Yap[1], Benjamin Simon Pickard[2], Sook Yee Gan[3], Elaine Wan Ling Chan[4]*

[1] School of Postgraduate Studies, International Medical University, Kuala Lumpur, Malaysia.

[2] Strathclyde Institute of Pharmacy and Biomedical Sciences, University of Strathclyde, Glasgow, G4 0RE, United Kingdom.

[3] Department of Life Sciences, School of Pharmacy, International Medical University, Kuala Lumpur, Malaysia.

[4] Institute for Research, Development and Innovation, International Medical University, Kuala Lumpur, Malaysia.

***Corresponding Author:**

Elaine Chan Wan Ling, Institute for Research, Development and Innovation, International Medical University, Jalan Jalil Perkasa 19, Bukit Jalil, 57000 Kuala Lumpur, Malaysia.

Phone: +60 3 2731 7718; E-mail: elainechan@imu.edu.my

Abstract

Alzheimer's disease is an irreversible neurodegenerative disease, which accounts for most dementia cases. Neuroinflammation is increasingly recognised for its roles in Alzheimer's disease pathogenesis which, in part, links amyloid-beta to neuronal death. Neuroinflammatory signalling can be exhibited by neurons themselves, potentially leading to widespread neuronal cell death, although neuroinflammation is commonly associated with glial cells.. The presence of the inflammasomes such as nucleotide-binding leucine-rich repeat receptors protein 1 in neurons accelerates amyloid-beta -induced neuroinflammation and has been shown to trigger neuronal pyroptosis in murine Alzheimer's disease models. However, the pathways involved in amyloid-beta activation of inflammasomes have yet to be elucidated.. In this study, a gene trap mutagenesis approach was utilised to resolve the genes functionally involved in inflammasome signalling within neurons, and the mechanism behind amyloid-beta-induced neuronal death. The results indicate that amyloid-beta significantly accelerated neuroinflammatory cell death in the presence of a primed inflammasome (the NLR family pyrin domain-containing 1). The mutagenesis screen discovered the atypical mitochondrial Ras homolog family member T1 as a significant contributor to amyloid-beta-induced inflammasome -mediated neuronal death. The mutagenesis screen also identified two genes involved in transforming growth factor beta signalling, namely Transforming Growth Factor Beta Receptor 1 and SNW domain containing 1. Additionally, a gene associated with cytoskeletal reorganisation, SLIT-ROBO Rho GTPase Activating Protein 3 was found to be neuroprotective. In conclusion, these genes could play important roles in inflammasome signalling in neurons, which makes them promising therapeutic targets for future drug development against neuroinflammation in Alzheimer's disease.

Keywords

Alzheimer's disease; neuroinflammation; NLRP1 inflammasome; gene trap mutagenesis; amyloid-beta

Abbreviations

AD: Alzheimer's disease

CNS: Central nervous system

Aβ: Amyloid-beta

MDP: Muramyl dipeptide

NLRP1: NLR family pyrin domain-containing 1NLRP3: NLR family pyrin domain-containing 3

SD: Splice donor

ARE: AU rich element

RACE: Rapid amplification of cDNA ends

NGS: Next-generation sequencing

Log FC: Log_2 fold change

PD: Parkinson's disease

Introduction

Alzheimer's disease (AD) is a neurodegenerative disease which progressively interferes with behaviour, cognition, and memory, ultimately leading to death. It is the most common form of dementia, accounting for approximately 60-80% of total dementia cases.

The estimated prevalence of AD is 10-30% in populations above 65 years old (Masters et al., 2015). Yet, the precise aetiology of the disease remains elusive and there is no available cure capable of reversing disease progression. Current AD therapies are primarily limited to symptom management and improvement of patient quality of life. As such, the race for the discovery of novel therapeutic targets for AD is now more crucial than ever. Recently, studies on the innate immunity within the central nervous system (CNS) are beginning to gain traction as neuroinflammation becomes widely suspected as the missing link between the two pathological hallmarks of AD (amyloid-β (Aβ) and neurofibrillary tangles) and neuronal death (Kinney et al., 2018). In particular, the regulatory molecules of inflammation known as inflammasomes could be responsible for neuroinflammation in AD as they enable an immune response against AD pathologies in both microglia and in neurons (Yap et al., 2019; Sarlus and Heneka, 2017). The activation of inflammasomes results in caspase-1 mediated pyroptosis, a form of autolytic cell death characterised by the rupture of the cell membrane followed by the release of pro-inflammatory cytokines (Bergsbaken et al., 2009). The roles of inflammasomes, especially NLR family pyrin domain-containing 3 (NLRP3), in AD have been widely implicated in glial cells, but not in neurons (Tan et al., 2013). However, if neurons are able to participate in inflammasome-mediated neuroinflammation, it could lead to widespread neuronal pyroptosis, resulting in permanent neuronal loss. Aβ has also been shown to activate the NLR family pyrin domain-containing 1 (NLRP1) inflammasome leading to neuronal pyroptosis in murine models (Tan et al., 2014). However, the precise mechanism of inflammasome activation by Aβ in neurons is currently unclear. Given that the main constituent inflammasome in human neurons is NLRP1 not NLRP3 (Kaushal et al., 2015; Walsh et al., 2014), a gene trap mutagenesis phenotypic screen approach has been utilised to investigate the molecular signalling pathways involved in Aβ induction of the NLRP1 inflammasome in a human neuron model.

Gene trap mutagenesis generates random insertional mutations via genomic integration of a gene trap plasmid vector. Originally used to generate mutant embryonic stem cells, gene trap mutagenesis has since undergone substantial development and found its usefulness in identification of novel gene functions and molecular mechanisms (Morris et al., 2018; Gow et al., 2013; Salminen et al., 1998). In this study, we employed pGTIV3, an advanced poly(A) trap vector containing a human β-actin promoter upstream of *neoR* gene and a rabbit β-globin-derived splice donor (SD) sequence (Tsakiridis et al., 2009). A unique feature of this vector is the inclusion of a synthetic intron with a *cis*-acting mRNA destabilising AU rich element (ARE) which degrades the transcribed Neomycin resistance (*neoR*) mRNA if expressed. In the event that the gene trap vector non-productively integrates into the genome outside of a gene, the synthetic intron is not removed resulting in the inclusion of the ARE which disintegrates the resulting *neoR* mRNA transcript and the cell does not gain resistance to neomycin selection. Only true SD splicing events resulting from disruptive vector insertion into a gene intron permit neomycin resistance under selection and incorporation of the mutant cell into the resulting library.

We introduced pGTIV3 into the SH-SY5Y neuroblastoma cell line genome to produce a library of cells which collectively represented approximately 15,000 different heterozygous gene mutations. In order to elucidate the biological pathways mediating Aβ-induced, inflammasome mediated neuronal death, the library cells were subjected to treatment with Aβ and/or muramyl dipeptide (MDP). MDP is a derivative of bacterial peptidoglycan which is used as an activating ligand for the NLRP1 inflammasome (Faustin et al., 2007). In addition to stimulating inflammasome oligomerisation, MDP encourages the formation of NOD2-NLRP1 complex to induce NLRP1-dependent caspase-1 processing (Hsu et al., 2008). The treatment-recovery selection process was repeated over 7 cycles, selecting for mutant cells with resistance to cell death. Rapid amplification of cDNA ends (RACE),

followed by targeted next-generation sequencing (NGS) were then performed to identify trapped genes. The identified genes represent significant regulators of the susceptibility of neurons to Aβ-induced inflammasome-mediated neuronal death.

Methods

Aβ and MDP preparation

Synthetic $A\beta_{1-42}$ peptide (Genscript, USA) was dissolved in dimethyl sulfoxide (DMSO) to a concentration of 5mM and further diluted to a 200 μM stock solution with phosphate buffer saline (PBS). This solution was incubated at 4ºC for 24 hours and stored at -20ºC until use. During the experiment, the Aβ was further diluted to a final concentration of 5,10, 20 and 40 μM in the samples. MDP (InvivoGen, USA) was prepared as a 10 mg/mL stock in endotoxin-free water. When used in experiments, the MDP was diluted to 100 μg/mL with serum-free media before further diluted in the samples to a final working concentration of 10 μg/mL (Chen et al., 2020).

Cell culture and treatments

SH-SY5Y neuroblastoma cells (ATCC® CRL-2266™, American Type Culture Collection (ATCC), Virginia, USA) were cultured in T25 flasks with at least 5mL of DMEM/F12 (1:1) culture media supplemented with GlutaMAX™ (Gibco, USA), 10% foetal bovine serum (Biosera, France) and 1% penicillin-streptomycin (Gibco, USA). The cells were incubated at 37ºC with 5% CO_2 in humidified air. The culture medium was replaced every two days. At 70% confluency, the cells were dissociated with TrypLE Express (Gibco, USA) and passaged in new T25 flasks. For cell treatment, serum-free cell culture media

consisted of DMEM/F12 supplemented with GlutaMAX^{TM} and 1% penicillin-streptomycin were used.

Throughout this study, the treatment regimens were conducted in four groups: Control (cells exposed to only serum-free media), Aβ (cells exposed to 20 μM Aβ), MDP (cells exposed to 10 μg/mL MDP) and Aβ+MDP (cells co-exposed to 20 μM Aβ and 10 μg/mL MDP).

Cell viability assay

Cell viability was measured using the RealTime-Glo MT™ Cell Viability Assay kit (Promega, USA). SH-SY5Y cells were seeded at the density of $3x10^4$ cells/well in a white opaque 96-well plate and incubated overnight. The serum-free media, MT Cell Viability Substrate and NanoLuc® Enzyme (components of the assay kit) were pre-warmed in a 37ºC water bath prior to preparation of a 2x concentration of enzyme-substrate mixture. Serum free media were used to arrest cell growth before performing this assay so that the cells in the control wells did not overgrow after 72 hours. The mixture was then added into the cell culture samples to a final concentration of 1x. The luminescence signal was measured with SpectraMAX M3 microplate reader at 2-hour time points for 72 hours. The assay was performed in six replicates for all the four treatment group (Control, Aβ, MDP and Aβ+MDP).

Prior to the treatment assays, cell viability assay was also conducted using various concentrations of Aβ (5, 10, 20 and 40 μM) to determine the concentration of Aβ which was used in the treatment groups (20 μM).

.

Western blot

For protein quantification, SH-SY5Y cells were seeded in 6-well plates ($2x10^6$ cells/well) and allowed to stabilise for 24 hours. The cells were then treated as described for 2 hours. Total protein in the cell lysate was harvested in RIPA buffer (Abcam, UK) and quantified using the Bradford assay (Bio-Rad, USA). Proteins were also separated using 10% sodium dodecyl sulphate polyacrylamide (SDS-PAGE) gel at 120V where each well was loaded with 30µg protein in Laemmli buffer (Bio-Rad, USA). The gel was blotted onto a polyvinylidene difluoride (PVDF) membrane. The membrane was then blocked with Blocking One (Nacalai Tesque, Japan) for one hour at room temperature. The proteins of interest in each sample were probed using primary antibodies (anti-NLRP1, anti-caspase-1 and anti-β-actin; Cell signalling Technology, USA) at 1:1000 dilution. β-actin was used as loading control. Anti-rabbit IgG HRP-conjugated antibody (Cell Signalling Technology, Massachusetts, USA) at 1:2000 was used as secondary antibody. The Chemi-Lumi One Super enhanced chemiluminescence reagent (Nacalai Tesque, Japan) was used to detect the blots. Blot visualization and densitometric analyses were performed using Bio-Rad Image Lab 6.0.1 software. All western blots were performed in triplicates.

Statistical analyses

The differences of means between the treatment groups were analysed with one-way analysis of variance (ANOVA) followed by Tukey's Honest Significant Difference post-hoc test. All statistical analyses were computed with GraphPad Prism 8.0.2 software.

Gene-trap mutagenesis and selection process

188 The pGTIV3 plasmid was linearised using the PvuI restriction enzyme and then
189 transfected into SH-SY5Y cells via nucleofection utilising Cell Line Nucleofector^{TM} Kit V
190 (Lonza, Switzerland), followed by G418/Geneticin selection for productive mutation events,
191 and expansion to produce multiple aliquots. The resulting library cells were seeded in T12.5
192 flasks ($5x10^5$ cells/flask), incubated overnight and treated as described for the four treatment
193 groups using 20 μM Aβ. Surviving populations of cells were allowed to recover to full
194 confluency before being re-seeded (excess cells archived as frozen stocks) and re-treated for
195 another 72 hours. This treatment-recovery process was performed for 7 cycles.

196

197 *First strand cDNA synthesis and RACE*

198 At the end of the 7 cycles of selection, the surviving cells were allowed to recover in
199 T75 flasks. At full confluency, the total RNA was extracted from these cells with ISOLATE
200 II RNA Mini Kit (Bioline, UK) according to the manufacturer's protocol. From the eluted
201 RNA, first strand cDNA was synthesised using SuperScript IV Reverse Transcriptase
202 (Invitrogen, USA). The modified oligo(dT) primer used for reverse transcription (3CDSynth)
203 was 5' AAG CAG TGG TAA CAA CGC AGA GTA CTT TTT TTT TTT TTT TTT
204 TTT TTT TTT TVN 3'.

205 We utilised the 3' RACE method to amplify *neoR* - mutant allele fusion transcripts in
206 the experimental and control groups for identification and quantification purposes. This took
207 advantage of the natural poly(A) tail as a functional priming site to attach an adaptor via the
208 modified oligo(dT) primer and produced a first strand cDNA with a known sequence (*neoR*)
209 at the 5' end. To ensure the specificity of the final amplicons, the cDNA strands were
210 amplified through a series of nested PCR steps utilising two sets of forward and reverse
211 primers (RACE#1 and RACE#2 primers). RACE#1 primers consisted of SD5-P1 (forward)

5’ GCT TGC CGA ATA TCA TGG TGG AAA ATG G 3’ and UPM (reverse) (UPM was a mixture of 0.4 µM UPL 5’ CTA ATA CGA CTC ACT ATA GGG CAA GCA GTG GTA ACA ACG CAG AGT 3’ and 2 µM UPS 5’ CTA ATA CGA CTC ACT ATA GGG C 3’). RACE#2 primers were SD5-P3 (forward) 5’ CGC ATC GCC TTC TAT CGC CTT CTT GAC G 3’ and Nest1 (reverse) 5’ AAG CAG TGG TAA CAA CGC AGA GT 3’. The thermal cycling parameters set were: 94 ºC for 5 minutes, (94 ºC for 30 seconds, 70 ºC for 30 seconds, 72 ºC for 3 minutes) x 5 cycles, (94ºC for 30 seconds, 68 ºC for 30 seconds, 72 ºC for 3 minutes) x 30 cycles, and finally 72 ºC for 5 minutes.

Library preparation and next generation sequencing

The amplicons were taken through library construction using the Illumina TruSeq Nano Library Prep kit. Paired-end targeted sequencing was performed with the Illumina NextSeq instrument which produced 75 bp reads for each end, totalling 30 million reads. Only the subset of transcripts produced by the gene trap insertional mutagenesis (neomycin resistance – mutated gene fusions) were sequenced. Because of the reduced genomic complexity, we opted to perform multiplex sequencing by incorporating ‘barcode’ sequences to each DNA fragment during library preparation to distinguish between samples and replicates within the amplicon pool (n = 3).

Bioinformatics analysis

NGS data analysis was conducted with the repository of Bioconductor tools available as GUI at the web-based Galaxy platform (https://usegalaxy.org/). The NGS data were available in FASTQ format compressed in gz files (fastq.gz). The FASTQ files were converted into FASTQ Sanger format (fastqsanger.gz) using the FASTQ Groomer tool in

order to ensure compatibility with the Galaxy platform (Blankenberg et al., 2010). The raw sequences were then mapped into the human genome (hg38) using the HISAT2 aligner with default parameters to produce BAM files outputs (Kim et al., 2015). The aligned sequences were then assembled into transcripts using StringTie transcript assembler (Pertea et al., 2015). An Ensembl hg38 gene annotation file was used to guide transcript assembly and only transcripts that matched the reference annotation file were accepted (The parameter 'Use Reference transcripts only?' was set to True). The assembler was also set to output a tabular file containing gene counts compatible with the limma-voom software package. Limma-voom analysis and data visualisation were performed on the Degust online platform (http://degust.erc.monash.edu/) (Law et al., 2014).

Results

MDP-primed inflammasome accelerates Aβ-induced SH-SY5Y cell death

Cells treated with 20 µM and 40 µM Aβ in serum-free conditions showed a progressive loss of cell viability over 72 hours (Fig. 1A). Since there was no difference in cell viability when exposed to 20 µM or 40 µM Aβ across most time points, 20 µM Aβ was used for subsequent experiments. Interestingly, when SH-SY5Y cells were exposed to Aβ (singly, or in combination with MDP), cell viability appeared to increase above the control level from the 4-hour time point and reached a peak at 18 hours, after which the cell viability sharply and steadily declined (Fig. 1B). The viability of cells treated with Aβ and Aβ+MDP fell below 100% after 36 hours with Aβ+MDP cells dying at a comparatively higher rate. Cells treated with MDP alone, however, showed no significant cell death throughout the duration of the assay. At the 72-hour time point, the viability of cells treated with Aβ dropped to 72%. Importantly, co-exposure of Aβ with MDP further decreased cell viability to 56%, implying

that Aβ and MDP-primed inflammasome functioned in synergy to promote neuroinflammatory cell death. The trend of cell viability post-treatment was supported by microscopic images (Fig. 2). At 24 hours, the morphology of SH-SY5Y cells was similar across the groups. However, at 48 hours, the morphology of the SH-SY5Y cells changed in the treatment groups, signifying the progress of cell death. Finally, at 72 hours, an even greater number of SH-SY5Y cells had changed morphologically when subjected to Aβ and Aβ+MDP treatments compared to control and MDP treatment alone. In order to maximise selection pressure in the gene trap mutagenesis screen, library cells were exposed to the respective treatments for 72 hours per cycle.

Aβ and MDP synergistically intensified NLRP1 activity in SH-SY5Y cells

In order to examine the effect of Aβ on the activity of NLRP1 inflammasome, the levels of NLRP1, inactive procaspase-1 and the P20 fragment of activated caspase-1 were measured after exposure of SH-SY5Y cells to the respective treatments for 2 hours. The activation of inflammasomes simultaneously triggers autophagic degradation of the inflammasome complex as a negative regulatory mechanism to limit inflammation (Sun et al., 2017; Shi et al., 2012). As such, NLRP1 and caspase-1 levels must be detected prior to their degradation. As shown in Fig. 3, Aβ by itself did not significantly affect the expression of NLRP1. Interestingly, however, Aβ treatment did induce caspase-1 activation and cleavage, as shown by a 2-fold increase in P20 fragments compared to control. MDP was able to induce a significant increase in intracellular NLRP1 levels. At the same time, exposure of SH-SY5Y cells to MDP resulted in significant increase in the expression and activation of caspase-1. However, a significant portion of caspase-1 remained in its inactive form. We then studied the capability of Aβ to exacerbate neuroinflammation in the presence of MDP-primed

NLRP1 activation. When cells were co-treated with MDP and Aβ, there was a remarkable surge in conversion of procaspase-1 into its activated form, as indicated by a 5.6-fold increase in P20 fragment generation compared to control.

Gene trap mutagenesis screen for signalling intermediates underlying Aβ-induced inflammasome-mediated neuronal death

Through a gene allele representation analysis, 13,605 mutated genes were identified when the False Discovery Rate (FDR) cut-off was set to 1.0 (all sequenced genes regardless of their differential representation level significance), which denotes the number of genes successfully targeted by the gene trap vector in the parent library. When an FDR cut-off of 0.05 was applied, seven mutated genes were returned with a significant allele representation of $\log_2$ fold change (log FC) more than 3 or less than -3 in one or more treatment groups (Table 1). The genes identified by the functional gene trap mutagenesis screen were considered to be important regulators of cell survivability under the different treatment conditions. It should be noted that the limma-voom software employed in this study could compute differential gene expression, which was measured as a proxy for read depth as the trapped genes were expressed at a constant rate driven by the gene trap vector's built-in β-actin promoter. The differences in read depth reflected the changes in cell fitness caused by each trapped gene. The higher the read depth for a particular gene, the greater number of cells in the surviving population carrying its mutation, and *vice versa*.

The mutation of a susceptibility gene would promote the survival of the mutant containing cells, hence reflected in sequence read depth with positive log FC (Table 1). Henceforth, these genes would be referred to as 'susceptibility genes', reflecting their 'wild type' susceptibility effect. As shown in Table 1, three susceptibility genes (*RHOT1*, *TGFBR1*

and *BEND5*) were identified with log FC > 3 (reduction of gene function leading to > 8 fold read depth increase in the treatment groups compared to control). The most significant susceptibility gene in Aβ+MDP group was *RHOT1*, as evidenced by its high gene trap representation (mutant gene log FC = 7.11). This was followed by *TGFBR1* which conferred susceptibility in almost equal capacity in all three treatment groups, with mutant gene log FC values of 3.29, 3.39 and 3.17 for Aβ, MDP and Aβ+MDP respectively (Table 1, Fig. 4). Interestingly, *BEND5* conferred susceptibility when subjected to treatment with MDP only (mutant gene log FC = 4.06) but not in the presence of Aβ.

Conversely, mutation of a naturally protective gene would result in reduced mutant cell survival, hence a read depth with negative log FC (Table 1). As shown in Table 1, four protective genes (*CNP*, *SNW1*, *GREB1* and *SRGAP3*) were identified with log FC < -3 (reduction of gene function leading to > 8 fold reduction in read depth in the treatment groups compared to control). The most significant protective gene observed was *CNP* (mutant gene log FC = -7.15), which was the only protective gene recorded in the Aβ+MDP group. *SNW1* was a common protective gene in Aβ and MDP groups, both with similar log FC (log FC = -3.08 and -3.34 respectively). However, *SRGAP3* was a protective gene unique to the Aβ group (mutant gene log FC = -4.82), while *GREB1* was unique to MDP group (mutant gene log FC = -3.73).

328 **Table 1 List of genes with significant changes in gene trap representation relative to**
329 **control. Significant 'wild type' susceptibility genes (log FC > 3) and 'wild-type'**
330 **protective genes (log FC < -3) are bolded.**

Gene name	FDR	P-value	Log FC		
			Aβ	**MDP**	**Aβ+MDP**
RHOT1	$3.14x10^{-3}$	$2.31x10^{-7}$	-0.11	0.11	**7.11**
CNP	0.02	$2.73x10^{-6}$	-0.01	0.09	**-7.15**
TGFBR1	0.02	$4.088x10^{-6}$	**3.29**	**3.39**	**3.17**
SNW1	0.03	$8.88x10^{-6}$	**-3.08**	**-3.34**	-0.11
BEND5	0.04	$1.83x10^{-5}$	-1.97	**4.06**	-0.81
GREB1	0.04	$1.95x10^{-5}$	0.43	**-3.73**	0.33
SRGAP3	0.04	$2.16x10^{-5}$	**-4.82**	-0.67	0.62

331

332

333

Discussion

Aβ is one of the major neurotoxic factors responsible for neurodegeneration in AD. Exposure to Aβ alone is sufficient to cause progressive neuronal death. Although Aβ is indeed neurotoxic by itself, the priming of neuronal inflammasomes, including NLRP1, by an external stimulus such as MDP (10 µg/ml) significantly aggravates neuronal death as shown by the drastic decrease in neuronal viability in Aβ+MDP treatment group (Fig. 1B). A study showed that MDP at 10 µg/ml induced the upregulation of phosphorylated-p38 mitogen-activated protein kinase (MAPK; Chen et al., 2020). In neurons, the MAPK signalling pathway plays an important role in the regulation of NLRP1 inflammasome expression and activation (Fann et al., 2018). Interestingly, however, MDP by itself did not cause a significant change in cell viability, suggesting that inflammasome activation alone did not result in immediate cell death. It was also unlikely that Aβ caused neuronal death via the NLRP1 inflammasome pathway as, by itself, it did not significantly elevate NLRP1 levels, having insufficient caspase-1 activity to trigger pyroptosis (Fig. 3). However, when neurons were co-exposed with MDP, Aβ was able to significantly elevate caspase-1 activity, resulting in a drastic loss of neuronal viability. These results suggest that, while inflammasome and caspase-1 activation does not necessarily lead to neuronal death, co-stimulation with an external inflammagenic substance could lead inflammasome signalling into an overdrive sufficient to induce pyroptosis, thus significantly accelerating cell death. Therefore, the exposure of the brain to immunogenic stimuli such as pathogens, which are increasingly recognised for their roles in AD (Miklossy, 2011), could drastically accelerate neuronal death via inflammasome activation and pyroptosis. Indeed, it was proposed that Aβ is deposited in the brain as part of an innate immune response against pathogenic infections (Moir et al., 2018). However, there is a limitation to the cell viability assay used in this study as serum

deprivation for extended duration could be a confounding stress factor to the cells. The observed effect needs to be further verified using *in vivo* models.

The random genomic mutagenesis generated by gene trapping is a useful tool to screen for molecular mechanisms underlying a biological process. Unlike other gene silencing tools, such as siRNA, gene traps produce a permanent heterozygous (monoallelic) knockout which is equivalent to 50% reduction in gene product expression (Gow et al., 2013). This is particularly advantageous as homozygous knockouts could be lethal, and human mutations are often heterozygous in nature. With FDR cut-off set to 0.05, the gene trap mutagenesis phenotypic screen discovered seven significant genes which could highlight the underlying signalling pathways regulating neuronal survival and death when subjected to Aβ and MDP-primed NLRP1 inflammasome. The most significant of these 'hit' genes are *RHOT1* and *CNP* with mutant allele representation of log FC = 7.11 ('wild-type' susceptibility) and -7.15 ('wild-type' protective) respectively in the Aβ+MDP group. Both *RHOT1* and *CNP* have roles in mitochondrial toxicity, presumably a crucial factor in Aβ-induced NLRP1-mediated neuronal death. The *RHOT1* gene encodes the Ras Homolog Family Member T1 protein, also known as Mitochondrial Rho GTPase 1 (MIRO1). MIRO1 is a member of the Rho family of GTPases, which in turn belongs to the Ras superfamily of small GTPases. Rho GTPases are typically small G proteins which are responsible for the regulation of many essential biological processes including cell growth, transcriptional regulation, membrane trafficking and cell motility (Hanna and El-Sibai, 2013; Aznar and Lacal, 2001). MIRO1 is essential in healthy neuronal function. Germline Miro1 knockout in the mouse resulted in perinatal death, and conditional knockout of neuronal Miro1 in a mouse model led to defects in mitochondria distribution and retrograde axonal mitochondrial movement, resulting in impaired motor neuron function (Nguyen et al., 2014). MIRO1 may also contribute to the pathogenesis of neurodegenerative diseases such as Parkinson's disease

(PD) (Devine et al., 2016). MIRO1 is known to interact with the PD-associated proteins, parkin and PINK1, where MIRO1 is phosphorylated by PINK1 and subsequently ubiquitinylated by parkin, leading to its degradation by proteasomes (Hsieh et al., 2016; van der Merwe et al., 2015). The degradation of MIRO1 causes an arrest in mitochondria trafficking which quarantines defective mitochondria and prevents them from causing further damage to neighbouring healthy mitochondria. This immobilisation of mitochondrial movement also facilitates its selective degradation via phagosomes and autolysosomes, a process known as mitophagy. Impaired MIRO1 degradation disrupts mitophagic clearance of defective mitochondria which may elevate the production of reactive oxygen species (ROS) leading to the activation of the NLRP3 inflammasome (Chen et al., 2017; Gao et al., 2015). Considering that MIRO1-mediated neurotoxicity was only observed at a significant level in the Aβ+MDP group, we hypothesize that Aβ and the NLRP1 inflammasome could synergistically induce neuronal death through mitochondria dysfunction as in PD. It is possible that lack of MIRO1 production in the library cells encourages mitophagic clearance of defective mitochondria and enablesd cell survival.

Conversely, the *CNP* gene which encodes 2',3'-cyclic nucleotide 3' phosphodiesterase (CNPase) is found to be highly protective against Aβ-induced NLRP1-mediated neurotoxicity as indicated by a log FC = -7.15 for mutant *CNP* in the Aβ+MDP group. In the 2',3'-cAMP-adenosine pathway, CNPase is found to convert 2',3'-cAMP to 2'-AMP which is further metabolized into adenosine (Jackson, 2011). Elevated adenosine confers neuroprotective effects against excitotoxic neuronal damage (Wardas, 2002). CNPase is also known to confer neuroprotection against mitochondria-induced toxicity. Specifically, CNPase regulates the opening of the mitochondrial permeability transition pore (mPTP), a Ca^{2+}-gated channel which is formed in mitochondria in response to Ca^{2+} overload or oxidative stress in order to increase the permeability of mitochondrial membrane (Baburina et al., 2015;

Krestinina et al., 2015). Open mPTP abruptly increases the permeability of mitochondrial inner membrane (which is usually almost impermeable to solutes or ions) to molecules up to 1,500 Da, leading to excessive mitochondrial swelling and cell death by apoptosis or necrosis (Lemasters et al., 2009). It is possible that mutation of *CNP* gene encourages the opening of mPTP in response to Ca^{2+} and ROS imbalance in the cells as a result of Aβ and MDP treatment.

The mutagenesis screen also identified two genes involved in TGF-β signalling, *TGFBR1* and *SNW1*. The *TGFBR1* gene encodes the TGF-β receptor type I (TGFBR1) protein which functions as a signal transduction component in TGF-β signalling. TGFBR1 is integrated to the perpetually activated TGFBR2 as a dimer which spans the entire cell membrane. Upon binding to extracellular ligands, principally TGF-β cytokines, TGFBR1 is phosphorylated by TGFBR2, which in turn phosphorylates the intracellular SMAD family of proteins, specifically receptor-regulated SMAD proteins (R-SMADs) which consists of SMAD2 and SMAD3 (Hata and Chen, 2016). Phosphorylated R-SMADs then accumulate into complexes with SMAD4 (a common SMAD or co-SMAD) which together act as transcription factors that signal the expression of target genes. As a negative regulatory mechanism for TGF-β signalling, the transcription factor SKI acts as a co-repressor which binds to SMAD2-4, forming a complex which negatively regulates TGF-β response (Xu et al., 2000). The SKI-interacting protein (SKIP), encoded by the *SNW1* gene, binds to SKI and antagonises its repressor effect, thereby releasing SMADs and allowing for their phosphorylation by TGFBR1, thus augmenting TGF-β signalling (Leong et al., 2001). Our functional screen showed that silencing *TGFBR1* enabled neuronal survival in all three treatment groups at similar log FC in allele representation (mutant gene Log FC +3, Table 1), suggesting that *TGFBR1* conferred susceptibility in response to toxic environment not specific to either Aβ or MDP toxicity. *SNW1*, however, show an opposing effect in Aβ and

MDP groups with similar log FC (mutant gene Log FC = -3, Table 1) but not in the Aβ+MDP group where there was no significant log FC compared to control, suggesting that activation of other pathways overrode the protective effects of *SNW1*. TGF-β signalling is a heterogenous signalling pathway that regulates many biological processes such as cell proliferation and immunity (Batlle and Massagué, 2019). The published roles of TGF-β signalling in neuroinflammation and AD have been conflicting. It has been reported to promote neuroinflammation in AD by encouraging the release of pro-inflammatory cytokines such as IL-1β and TNF-α in microvessels isolated from AD cortex (Grammas and Ovase, 2002) and blocking TGF-β and its downstream SMAD2/3 signalling attenuates AD pathology (Town et al., 2008). Other studies have indicated that TGF-β is instead protective in nature, and its deficiency promotes neurodegeneration in AD (Tesseur et al., 2006). Further studies are required to evaluate the impact of TGF-β signalling, as well as its individual components, in neuroinflammation and AD pathogenesis.

Apart from *TGFBR1* and *SNW1*, the functional screen identified *SRGAP3* as a protective gene unique to the Aβ group. The *SRGAP3* gene encodes the Slit-Robo Rho GTPase Activating Protein 3 (srGAP3), also known as WAVE-Associated Rac GTPase Activating Protein (WRP) or Mental Disorder-Associated GTPase Activating Protein (MEGAP), which belongs to the Rho GAP family of Rho GTPase negative regulators. srGAP3 is involved in a variety of processes which are crucial for neuronal morphogenesis, axon guidance and synaptic functions (Huang et al., 2017). srGAP3 possibly confers neuroprotection against Aβ toxicity by regulating cytoskeletal reorganisation or participating in Slit-Robo signalling, both of which are vital for neurodevelopment and healthy cognitive functions (Bacon et al., 2013). However, this neuroprotective effect is nullified in the presence of MDP, suggesting that the activation of NLRP1 inflammasome perturbs srGAP3 function and probably the regulation of cytoskeletal dynamics, which drastically reduces

cellular rigidity against toxicity. This could have contributed to the synergism between Aβ and MDP-primed NLRP1 inflammasome in inducing severe loss of neuronal viability in the Aβ+MDP group.

BEND5 and *GREB1* showed significance in the MDP treatment group only, suggesting that exposure to Aβ negated the effects exerted by these genes. As with *SNW1, BEND5* is involved in DNA/RNA biding and transcription regulation. The *BEND5* gene encodes the protein BEN domain-containing protein 5. The mammalian BEND5 is a protein that contains a single BEN domain and is expressed in particularly high levels in pyramidal neurons (Dai et al., 2013). It functions as a transcriptional repressor and is likely involved neurogenesis by regulating the Notch signalling pathway. The *GREB1* gene codes for the growth-regulating oestrogen receptor binding 1 protein. *GREB1* is typically expressed upon binding of oestrogen response elements on oestrogen receptor 1 (ESR1) upstream of *GREB1* promoter (Sun et al., 2007).Treatment with MDP alone did not result in significant loss of neuronal viability. It was possible that the effects of these mutant genes under MDP treatment affected cell proliferation rates rather than inducing neurodegeneration.

While the gene trap mutagenesis screening provides a convenient and high-throughput method for preliminary elucidation of biological pathways, screen efficiency is potentially limited by several factors. Firstly, the efficiency of gene trap integration is dependent on the initial nucleofection process. Secondly, although pGTIV3 does not display a 3' intron bias, its inherent requirement for intronic integration means that genes that lack, or contain very small, introns may escape trapping. This presents a major challenge in unbiased genome-wide mutagenesis by achieving complete genome saturation. Finally, the mutagenesis screen does not inform the order of gene activities and pathways involved - whether they occur upstream or downstream of NLRP1 inflammasome activation by Aβ.

Conclusion

We have demonstrated that neuronal response to Aβ is augmented when NLRP1 inflammasomes are primed by an external, immunogenic factor, suggesting that glia-independent neuroinflammation could result in significant neuronal self-destruction, likely via pyroptosis. Based on the genes identified by the mutagenesis screen, several putative pathways are identified which could be involved in regulating neuronal death in AD conditions, particularly in an NLRP1-primed state. We hypothesise that Aβ and inflammasome could induce mitochondria toxicity similar to that observed in PD. Additionally, the mutagenesis screen could detect alterations in TGF-β signalling which might play a role in neuroinflammation in AD. For future studies, it is recommended that these genes be targeted for knockout via other gene editing tools such as the CRISPR-cas9 system, or small molecule inhibitors where available, to validate the function of these genes. It is also imperative to test the effects of the identified genes and pathways in more complex models such as neuron-glia co-cultures or *in vivo* models, which would more accurately represent neuroinflammatory and AD conditions. The gene trap mutagenesis approach also presents a powerful tool in elucidating biological pathways and gene function especially if utilised in tandem with other gene expression or protein binding assessment techniques such as the GAL4/UAS system, which allows the study of specific gene function by targeted expression (Brand and Perrimon, 1993), and targeted DamID (TaDa), which offers sensitive and cell type-specific transcriptional profiling without requiring cell isolation, cell sorting, fixation, or affinity purification (Southall et al., 2013). These techniques would be able to identify, in addition of novel signalling pathways, the genome-wide expression and interactions between genes in a particular pathway, which would undoubtedly prove to be

highly advantageous for the identification and development of novel therapeutic targets for AD.

Data statement

The datasets used and/or analysed during the current study are available from the corresponding author on reasonable request.

Competing interests

The authors declare that they have no competing interests.

Funding

This work was supported by the Fundamental Research Grant Scheme, Ministry of Higher Education of Malaysia (FRGS/1/2016/SKK08/IMU/03/1).

Authors' Contributions

EWLC, SYG and BSP designed the study. JKYY and BSP performed the experiments. JKYY wrote the manuscript. EWLC, SYG, BSP and JKYY contributed to the final edition of the manuscript.

Acknowledgment

We would like to thank Glasgow Polyomics, University of Glasgow for their services in library preparation and NGS.

References

Aznar, S., Lacal, J.C., 2001. Rho signals to cell growth and apoptosis. Cancer Lett. 165, 1–10. https://doi.org/10.1016/S0304-3835(01)00412-8

Baburina, Y., Azarashvili, T., Grachev, D., Krestinina, O., Galvita, A., Stricker, R., Reiser, G., 2015. Mitochondrial 2′, 3′-cyclic nucleotide 3′-phosphodiesterase (CNP) interacts with mPTP modulators and functional complexes (I-V) coupled with release of apoptotic factors. Neurochem. Int. 90, 46–55. https://doi.org/10.1016/j.neuint.2015.07.012

Bacon, C., Endris, V., Rappold, G.A., 2013. The cellular function of srGAP3 and its role in neuronal morphogenesis. Mech. Dev. 130, 391–395. https://doi.org/10.1016/j.mod.2012.10.005

Batlle, E., Massagué, J., 2019. Transforming Growth Factor-β Signaling in Immunity and Cancer. Immunity. 50, 924-940. https://doi.org/10.1016/j.immuni.2019.03.024

Bergsbaken, T., Fink, S.L., Cookson, B.T., 2009. Pyroptosis: Host cell death and inflammation. Nat. Rev. Microbiol. 7, 99–109. https://doi.org/10.1038/nrmicro2070

Blankenberg, D., Gordon, A., Von Kuster, G., Coraor, N., Taylor, J., Nekrutenko, A., Team, G., 2010. Manipulation of FASTQ data with galaxy. Bioinformatics 26, 1783–1785. https://doi.org/10.1093/bioinformatics/btq281

Brand, A.H., Perrimon, N., 1993. Targeted gene expression as a means of altering cell fates and generating dominant phenotypes. Development 118, 401–415.

549 Chen, L., Liu, C., Gao, J., Xie, Z., Chan, L.W.C., Keating, D.J., Yang, Y., Sun, J., Zhou, F.,
550 Wei, Y., Men, X., Yang, S., 2017. Inhibition of Miro1 disturbs mitophagy and
551 pancreatic β-cell function interfering insulin release via IRS-Akt-Foxo1 in diabetes.
552 Oncotarget. 8, 90693-90705. https://doi.org/10.18632/oncotarget.20963

553 Chen, Y., Chan, Y., Chen, W., Li, Y., Zhang, C., 2020. Muramyl dipeptide promotes Aβ1-42
554 oligomer production via the NOD2/p-p38 MAPK/BACE1 signaling pathway in the SH-
555 SY5Y cells. J. Integr. Neurosci. 19, 421-428.

556 Dai, Q., Ren, A., Westholm, J.O., Serganov, A.A., Patel, D.J., Lai, E.C., 2013. The BEN
557 domain is a novel sequence-specific DNA-binding domain conserved in neural
558 transcriptional repressors. Genes Dev. 27, 602–614.
559 https://doi.org/10.1101/gad.213314.113

560 Devine, M.J., Birsa, N., Kittler, J.T., 2016. Miro sculpts mitochondrial dynamics in neuronal
561 health and disease. Neurobiol. Dis. 90, 27–34. https://doi.org/10.1016/j.nbd.2015.12.008

562 Fann, D.Y., Lim, Y., Cheng, Y., Lok, K., Chunduri, P., Baik, S.Drummond, G.R., Dheen,
563 S.T., Sobey, C.G., Jo, D., Chen, C.L., Arumugam, T.V., 2018. Evidence that NF-κB and
564 MAPK Signaling Promotes NLRP Inflammasome Activation in Neurons Following
565 Ischemic Stroke. Mol. Neurobiol. 55, 1082-1096.

566 Faustin, B., Lartigue, L., Bruey, J.M., Luciano, F., Sergienko, E., Bailly-Maitre, B.,
567 Volkmann, N., Hanein, D., Rouiller, I., Reed, J.C., 2007. Reconstituted NALP1
568 Inflammasome Reveals Two-Step Mechanism of Caspase-1 Activation. Mol. Cell 25,
569 713–724. https://doi.org/10.1016/j.molcel.2007.01.032

570 Gao, J., Sang, M., Zhang, X., Zheng, T., Pan, J., Dai, M., Zhou, L., Yang, S., 2015. Miro1-
571 mediated mitochondrial dysfunction under high nutrient stress is linked to NOD-like
572 receptor 3 (NLRP3)-dependent inflammatory responses in rat pancreatic beta cells. Free

573 Radic. Biol. Med. 89, 322–332. https://doi.org/10.1016/j.freeradbiomed.2015.09.002

574 Gow, M., Mirembe, D., Longwe, Z., Pickard, B.S., 2013. A gene trap mutagenesis screen for
575 genes underlying cellular response to the mood stabilizer lithium. J. Cell. Mol. Med. 17,
576 657–663. https://doi.org/10.1111/jcmm.12048

577 Grammas, P., Ovase, R., 2002. Cerebrovascular transforming growth factor-β contributes to
578 inflammation in the Alzheimer's disease brain. Am. J. Pathol. 160, 1583-1587.
579 https://doi.org/10.1016/S0002-9440(10)61105-4

580 Hanna, S., El-Sibai, M., 2013. Signaling networks of Rho GTPases in cell motility. Cell.
581 Signal. 25, 1955–1961. https://doi.org/10.1016/j.cellsig.2013.04.009

582 Hata, A., Chen, Y.G., 2016. TGF-β signaling from receptors to smads. Cold Spring Harb.
583 Perspect. Biol. 8, a022061. https://doi.org/10.1101/cshperspect.a022061

584 Hsieh, C.H., Shaltouki, A., Gonzalez, A.E., Bettencourt da Cruz, A., Burbulla, L.F., St.
585 Lawrence, E., Schüle, B., Krainc, D., Palmer, T.D., Wang, X., 2016. Functional
586 Impairment in Miro Degradation and Mitophagy Is a Shared Feature in Familial and
587 Sporadic Parkinson's Disease. Cell Stem Cell 19, 709–724.
588 https://doi.org/10.1016/j.stem.2016.08.002

589 Hsu, L.C., Ali, S.R., McGillivray, S., Tseng, P.H., Mariathasan, S., Humke, E.W., Eckmann,
590 L., Powell, J.J., Nizet, V., Dixit, V.M., Karin, M., 2008. A NOD2-NALP1 complex
591 mediates caspase-1-dependent IL-1β secretion in response to Bacillus anthracis infection
592 and muramyl dipeptide. Proc. Natl. Acad. Sci. U. S. A. 105, 7803–7808.
593 https://doi.org/10.1073/pnas.0802726105

594 Huang, G.H., Sun, Z.L., Li, H.J., Feng, D.F., 2017. Rho GTPase-activating proteins:
595 Regulators of Rho GTPase activity in neuronal development and CNS diseases. Mol.

Cell. Neurosci. 80, 18–31. https://doi.org/10.1016/j.mcn.2017.01.007

Jackson, E.K., 2011. The 2',3'-cAMp-adenosine pathway. Am. J. Physiol. - Ren. Physiol. 301, f1160-1167. https://doi.org/10.1152/ajprenal.00450.2011

Kaushal, V., Dye, R., Pakavathkumar, P., Foveau, B., Flores, J., Hyman, B., Ghetti, B., Koller, B.H., LeBlanc, A.C., 2015. Neuronal NLRP1 inflammasome activation of Caspase-1 coordinately regulates inflammatory interleukin-1-beta production and axonal degeneration-associated Caspase-6 activation. Cell Death Differ. 22, 1676–1686. https://doi.org/10.1038/cdd.2015.16

Kim, D., Langmead, B., Salzberg, S.L., 2015. HISAT: A fast spliced aligner with low memory requirements. Nat. Methods 12, 357–360. https://doi.org/10.1038/nmeth.3317

Kinney, J.W., Bemiller, S.M., Murtishaw, A.S., Leisgang, A.M., Salazar, A.M., Lamb, B.T., 2018. Inflammation as a central mechanism in Alzheimer's disease. Alzheimer's Dement. Transl. Res. Clin. Interv. 4, 575–590. https://doi.org/10.1016/j.trci.2018.06.014

Krestinina, O., Azarashvili, T., Baburina, Y., Galvita, A., Grachev, D., Stricker, R., Reiser, G., 2015. In aging, the vulnerability of rat brain mitochondria is enhanced due to reduced level of 2′,3′-cyclic nucleotide-3′-phosphodiesterase (CNP) and subsequently increased permeability transition in brain mitochondria in old animals. Neurochem. Int. 80, 41–50. https://doi.org/10.1016/j.neuint.2014.09.008

Law, C.W., Chen, Y., Shi, W., Smyth, G.K., 2014. Voom: Precision weights unlock linear model analysis tools for RNA-seq read counts. Genome Biol. 15, R29.https://doi.org/10.1186/gb-2014-15-2-r29

Lemasters, J.J., Theruvath, T.P., Zhong, Z., Nieminen, A.L., 2009. Mitochondrial calcium and the permeability transition in cell death. Biochim. Biophys. Acta - Bioenerg. 1787,

1395–1401. https://doi.org/10.1016/j.bbabio.2009.06.009

Leong, G.M., Subramaniam, N., Figueroa, J., Flanagan, J.L., Hayman, M.J., Eisman, J.A., Kouzmenko, A.P., 2001. Ski-interacting Protein Interacts with Smad Proteins to Augment Transforming Growth Factor-β-dependent Transcription. J. Biol. Chem. 276, 18243–18248. https://doi.org/10.1074/jbc.M010815200

Masters, C.L., Bateman, R., Blennow, K., Rowe, C.C., Sperling, R.A., Cummings, J.L., 2015. Alzheimer's disease. Nat. Rev. Dis. Prim. 1, 15056. https://doi.org/10.1038/nrdp.2015.56

Miklossy, J., 2011. Emerging roles of pathogens in Alzheimer disease. Expert Rev. Mol. Med. 13, e30. https://doi.org/10.1017/s1462399411002006

Moir, R.D., Lathe, R., Tanzi, R.E., 2018. The antimicrobial protection hypothesis of Alzheimer's disease. Alzheimer's Dement. 14, 1602–1614. https://doi.org/10.1016/j.jalz.2018.06.3040

Morris, S.M., Mhyre, A.J., Carmack, S.S., Myers, C.H., Burns, C., Ye, W., Ferrer, M., Olson, J.M., Klinghoffer, R.A., 2018. A modified gene trap approach for improved high-throughput cancer drug discovery. Oncogene 37, 4226–4238. https://doi.org/10.1038/s41388-018-0274-4

Nguyen, T.T., Oh, S.S., Weaver, D., Lewandowska, A., Maxfield, D., Schuler, M.H., Smith, N.K., Macfarlane, J., Saunders, G., Palmer, C.A., Debattisti, V., Koshiba, T., Pulst, S., Feldman, E.L., Hajnóczky, G., Shaw, J.M., 2014. Loss of Miro1-directed mitochondrial movement results in a novel murine model for neuron disease. Proc. Natl. Acad. Sci. U. S. A. 111, e3631-e3640. https://doi.org/10.1073/pnas.1402449111

Pertea, M., Pertea, G.M., Antonescu, C.M., Chang, T.C., Mendell, J.T., Salzberg, S.L., 2015.

642 StringTie enables improved reconstruction of a transcriptome from RNA-seq reads. Nat.
643 Biotechnol. 33, 290–295. https://doi.org/10.1038/nbt.3122

644 Salminen, M., Meyer, B.I., Gruss, P., 1998. Efficient poly a trap approach allows the capture
645 of genes specifically active in differentiated embryonic stem cells and in mouse
646 embryos. Dev. Dyn. 212, 326–333. https://doi.org/10.1002/(SICI)1097-
647 0177(199806)212:2<326::AID-AJA17>3.0.CO;2-1

648 Sarlus, H., Heneka, M.T., 2017. Microglia in Alzheimer's disease. J. Clin. Invest. 127, 3240–
649 3249. https://doi.org/10.1172/JCI90606

650 Shi, C.S., Shenderov, K., Huang, N.N., Kabat, J., Abu-Asab, M., Fitzgerald, K.A., Sher, A.,
651 Kehrl, J.H., 2012. Activation of autophagy by inflammatory signals limits IL-1β
652 production by targeting ubiquitinated inflammasomes for destruction. Nat. Immunol. 13,
653 255–263. https://doi.org/10.1038/ni.2215

654 Southall, T.D., Gold, K.S., Egger, B., Davidson, C.M., Caygill, E.E., Marshall, O.J., Brand,
655 A.H., 2013. Cell-type-specific profiling of gene expression and chromatin binding
656 without cell isolation: Assaying RNA pol II occupancy in neural stem cells. Dev. Cell
657 26, 101–112. https://doi.org/10.1016/j.devcel.2013.05.020

658 Sun, J., Nawaz, Z., Slingerland, J.M., 2007. Long-range activation of GREB1 by estrogen
659 receptor via three distal consensus estrogen-responsive elements in breast cancer cells.
660 Mol. Endocrinol. 21, 2651–2662. https://doi.org/10.1210/me.2007-0082

661 Sun, Q., Fan, J., Billiar, T.R., Scott, M.J., 2017. Inflammasome and autophagy regulation: A
662 two-way street. Mol. Med. 23, 188–195. https://doi.org/10.2119/molmed.2017.00077

663 Tan, M.S., Tan, L., Jiang, T., Zhu, X.C., Wang, H.F., Jia, C.D., Yu, J.T., 2014. Amyloid-β
664 induces NLRP1-dependent neuronal pyroptosis in models of Alzheimer's disease. Cell

Death Dis. 5, e1382. https://doi.org/10.1038/cddis.2014.348

Tan, M.S., Yu, J.T., Jiang, T., Zhu, X.C., Tan, L., 2013. The NLRP3 inflammasome in alzheimer's disease. Mol. Neurobiol. 48, 875–882. https://doi.org/10.1007/s12035-013-8475-x

Tesseur, I., Zou, K., Esposito, L., Bard, F., Berber, E., Van Can, J., Lin, A.H., Crews, L., Tremblay, P., Mathews, P., Mucke, L., Masliah, E., Wyss-Coray, T., 2006. Deficiency in neuronal TGF-β signaling promotes neurodegeneration and Alzheimer's pathology. J. Clin. Invest. 116, 3060–3069. https://doi.org/10.1172/JCI27341

Town, T., Laouar, Y., Pittenger, C., Mori, T., Szekely, C.A., Tan, J., Duman, R.S., Flavell, R.A., 2008. Blocking TGF-β-Smad2/3 innate immune signaling mitigates Alzheimer-like pathology. Nat. Med. 14, 681-687. https://doi.org/10.1038/nm1781

Tsakiridis, A., Tzouanacou, E., Rahman, A., Colby, D., Axton, R., Chambers, I., Wilson, V., Forrester, L., Brickman, J.M., 2009. Expression-independent gene trap vectors for random and targeted mutagenesis in embryonic stem cells. Nucleic Acids Res. 37, e129. https://doi.org/10.1093/nar/gkp640

van der Merwe, C., Jalali Sefid Dashti, Z., Christoffels, A., Loos, B., Bardien, S., 2015. Evidence for a common biological pathway linking three Parkinson's disease-causing genes: Parkin, PINK1 and DJ-1. Eur. J. Neurosci. 41, 1113-1125. https://doi.org/10.1111/ejn.12872

Walsh, J.G., Muruve, D.A., Power, C., 2014. Inflammasomes in the CNS. Nat. Rev. Neurosci. 15, 84–97. https://doi.org/10.1038/nrn3638

Wardas, J., 2002. Neuroprotective role of adenosine in the CNS. Pol. J. Pharmacol. 54, 313-326.

688 Xu, W., Angelis, K., Danielpour, D., Haddad, M.M., Bischof, O., Campisi, J., Stavnezer, E.,
689 Medrano, E.E., 2000. Ski acts as a co-repressor with Smad2 and Smad3 to regulate the
690 response to type β transforming growth factor. Proc. Natl. Acad. Sci. U. S. A. 97, 5924–
691 5929. https://doi.org/10.1073/pnas.090097797

692 Yap, J.K.Y., Pickard, B.S., Chan, E.W.L., Gan, S.Y., 2019. The Role of Neuronal NLRP1
693 Inflammasome in Alzheimer's Disease: Bringing Neurons into the Neuroinflammation
694 Game. Mol. Neurobiol. 56, 7741-7753. https://doi.org/10.1007/s12035-019-1638-7

695

696

697

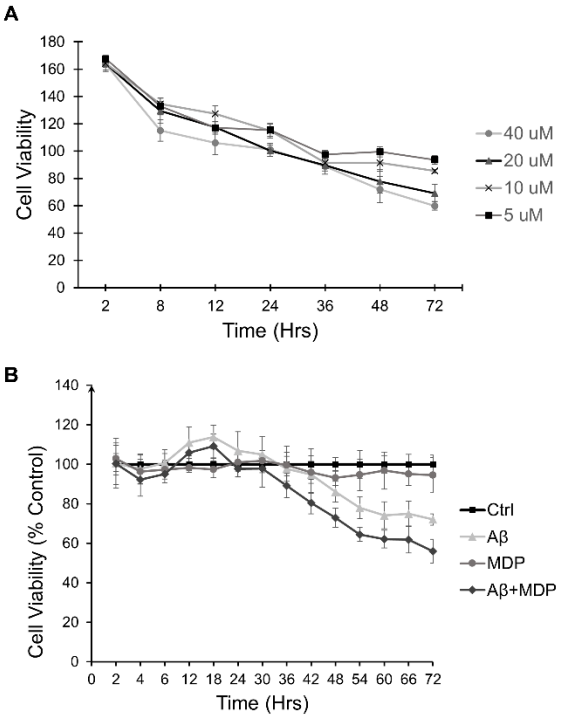

Figure 1 A) SH-SY5Y cell viability treated with 5, 10, 20 and 40µM Aβ measured in real time over 72 hours. B) SH-SY5Y cell viability in each treatment group compared to control, measured in real time over 72 hours. Control (only serum-free media), Aβ (amyloid-beta; 20µM Aβ), MDP (Muramyl dipeptide;10µg/mL) and Aβ+MDP (20µM Aβ and 10µg/mL MDP). To allow the assay to stabilise, the luminescent signal was measured after two hours after addition of reagents. Data are presented as mean ± SD (n = 6).

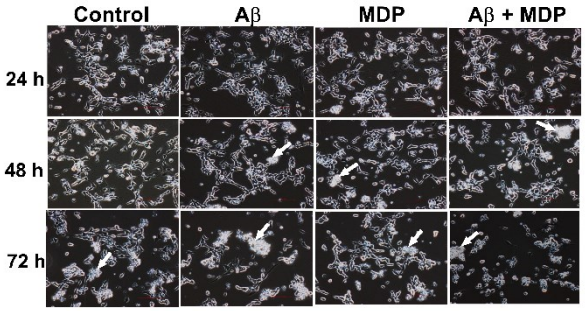

Figure 2 Morphology observed under phase-contrast microscopy of SH-SY5Y cells in control and treatment groups over 72 hours: Control (only serum-free media), Aβ (amyloid-beta; 20µM Aβ), MDP (Muramyl dipeptide;10µg/mL) and Aβ+MDP (20µM Aβ and 10µg/mL MDP). . Arrow indicates the morphological changes observed in SH-SY5Y cells following treatment with Aβ and/or MDP at 48 hours and 72 hours. Images are captured at 200x magnification (n = 3, three fields were taken for each sample).

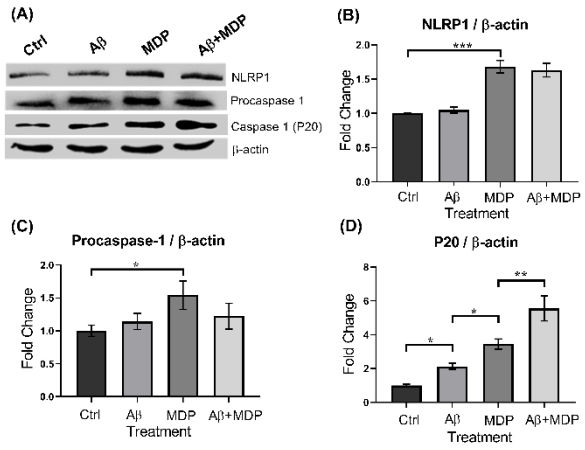

Figure 3 (A) Western blot of NLRP1 and caspase-1 normalized against β-actin. The proteins were quantified from total protein harvested from the cell lysates. (B-D)

Corresponding densitometric analyses. The data are presented as mean ± SD (n = 3). * denotes P < 0.05, ** denotes P < 0.005, * denotes P < 0.0005.**

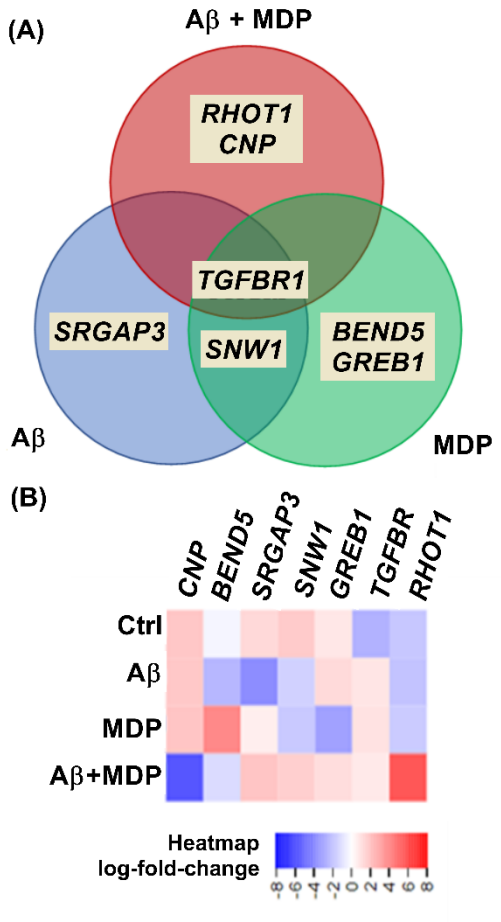

Figure 4 (A) Venn diagram depicting the significant genes (FDR cut-off = 0.05) contributing to neuronal survival or death in each treatment group compared to control. The overlapping sections indicate the genes common to multiple pair-wise

comparisons between groups. (B) Heatmap representative of changes in allele frequency of significant 'hit' genes in surviving mutant cell population across treatment groups.